Stark Effect on InP-InGaAs Separate Absorption and Multiplication Avalanche Photodiodes

Muhammad Navid Anjum Aadit[1] and Ummay Sumaya Khan[2]
Department of Electrical and Electronic Engineering
Bangladesh University of Engineering and Technology
Dhaka-1205, Bangladesh
Email: [1]navidanjumaadit@gmail.com and [2]ummay.sumaya@gmail.com

***Abstract*—We present electro-optical effects on Separate Absorption and Multiplication (SAM) Avalanche Photodiodes (APDs) with the presence of an external electric field. This effect is the well-known Stark Effect. We present optical shifts of SAM APDs with electric field variation and find that photons with lower energy can be absorbed to generate high photocurrent if Stark Effect is present. We demonstrate the change in absorption coefficient and exciton peak behavior with Stark Effect. We also present Stark Effect on photocurrent of SAM APDs by showing variation of responsivity. We use an in-house built Poisson-Schrödinger solver to simulate InP-InGaAs SAM APDs, as example. Thus, in this paper, we introduce a novel way to control and improve photocurrent of SAM APDs that can be extended to other APDs and used in optical modulators.**

***Keywords*—Absorption Coefficient, APD, Avalanche, SAM, Stark Effect**

I. Introduction

A photodiode is a semiconductor device similar to diodes that takes light as input and produces current as input which is generated by absorption of photons in the photodiode [1]. Avalanche Photodiode (APD) is a photodiode with high sensitivity which applies a reverse bias through avalanche multiplication to obtain high speed and gain [2]. APDs deliver higher signal to noise ratio than PIN photodiodes [3] and are widely used in optical rangefinders [4], spatial linearity correction [5] and scintillation detectors [6]. Group III-V compound based APDs have been improved to Separate Absorption and Multiplication (SAM) APDs where multiplication is provided by one type of carrier by separating the absorption and multiplication region [7].

SAM APDs have been developed for the use at communication wavelengths and so many researches have been done on these devices so far. They are used to convert optical signals into electrical signals. So it is essential to characterize SAM APDs correctly [8]. Notable improvement in terms of speed, efficiency and responsivity of APDs with the micro cavity is observed [9]. Performance analysis has been conducted on 8×8 APD arrays developed from large area (16 mm) APDs. This design of array was generated using a novel reverse etching technology [10]. The use of optical receivers to differentiate single photon excited avalanche events from dark current excited events is demonstrated based on Single Carrier Multiplication (SCM) APDs [11]. 7 dB optimal gain is possible using APD receivers in contrast with positive intrinsic negative receivers [12]. It is possible to obtain the APD receivers comparable with EMI receivers using time domain method [13]. The SNR (Signal to Noise Ratio) in APD photodiodes are also discussed and calculated in detail [14]. The effect of temperature on the value of optimal gain of APDs is less negligible than that of the turbulence; however, in both cases of turbulence channels APD receiver can be useful for overall improvement [15]. Moreover, the frequency response of SAM APDs is obtained considering the wavelength of the light [16]. Using the knowledge of Quantum-Confined Stark Effect, some multiple quantum well PIN and resonant cavity enhance (RCE) photodiodes are tuned [17],[18]. But to the best of our knowledge, Stark Effect on SAM APDs has not been reported yet experimentally or by simulation. In this work, we introduce a quantum mechanical self-consistent in-house built Poisson-Schrödinger solver along with Non Equilibrium Green Function (NEGF) approach to demonstrate Stark Effect on SAM APDs for the first time. The novelty of this work lies in the study of electro-optical shifts of SAM APDs due to Stark Effect and can be extended to Separate Absorption, Grading and Multiplication (SAGM) APDs [19].

Stark Effect describes the change in light spectrum on the application of an external electric field. Stark Effect may shift the energy to values lower than the gap [20]. In communication, high speed and low power optical modulators use Stark Effect extensively [21]. In this paper, we present electro-optical simulation results to show Stark Effect on SAM APDs with applied electric field. We simulate InGaAs-InP SAM APD device in COMSOL linked with MATLAB to obtain self-consistent Poisson-Schrödinger solution and show the variation absorption coefficient with the applied electric field. Moreover, we present shift of peak exciton energy in presence of that field. Finally, we present photocurrent and responsivity variation along with wavelengths due to Stark Effect. Demonstration of Stark Effect mechanisms on SAM APDs could open up many new possibilities for optical modulators and solid state photomultipliers [22].

978-1-5090-1269-5/16/$31.00 ©2016 IEEE

II. Device Structure and Modeling

A. Device Structure

Fig. 1 shows the simplified schematic of an InGaAs-InP APD with separate absorption and multiplication (SAM) region [23]. The p and n type doping of InP are denoted by capital letters, P and N. InP has a wider bandgap than InGaAs. The main depletion layer is between P^+-InP and N-InP layer. In the N-InP layer, avalanche multiplication takes place as the field is greatest there. The field in the n-InGaAs is weaker and the depletion region of this layer reaches through to the N-InP layer with sufficient reverse bias. Photons pass through the InP layer and they are absorbed in the n-InGaAs layer. Drift by the field takes the carriers to the avalanche region where they are multiplied.

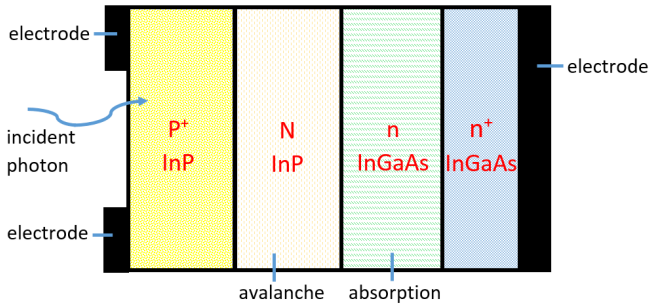

Fig. 1. Schematic Model of an InGaAs-InP SAM APD

B. Modeling

We simulate the device shown in Fig. 1 in COMSOL Multiphysics linked with MATLAB using a 3D Poisson-2D Schrödinger solver. The solver is self-consistent and built based on the technique described in [24]. We calculate net charge in the device using Fast Uncoupled Mode (FUMS) approach and then photocurrent by Non Equilibrium Green Function (NEGF) approach.

Poisson's equation can be described by:

$$-\nabla(\varepsilon\nabla U) = \rho, \tag{1}$$

where,
$\nabla \equiv \left(\hat{x}\frac{d}{dx} + \hat{y}\frac{d}{dy} + \hat{z}\frac{d}{dz}\right)$,
U is the electrostatic potential,
ρ is the charge density,
ε is the permittivity.

If the optical input power is P_{in}, then at distance d, we can calculate the optical output power as $P(d)$:

$$P(d) = P_{in}(1 - e^{-\alpha_s(\lambda)d}), \tag{2}$$

where, $\alpha_s(\lambda)$ is absorption coefficient.

In terms of energy gap, we can express the wavelength above which cut-off occurs as:

$$\lambda_{cut}(\mu\text{m}) = \frac{1.24}{E_g(\text{eV})}, \tag{3}$$

where, E_g is bandgap of the semiconductor material used.

The absorbed power in the depletion region at distance d can be also expressed considering reflectivity as:

$$(1 - r_f)P(d) = P_{in}(1 - e^{-\alpha_s(\lambda)d})(1 - r_f), \tag{4}$$

where, r_f is entrance face reflectivity.

As a result, the primary absorption photocurrent is:

$$I_p = \frac{q}{h\nu}P_{in}(1 - e^{-\alpha_s(\lambda)d})(1 - r_f), \tag{5}$$

where, q is charge of electron,
h is Planck's constant and
ν is frequency of incident photon.

The current gain M which is also known as multiplication factor of a photodiode can be expressed as:

$$M = \frac{I_o}{I_p}, \tag{6}$$

where, I_p is the primary photocurrent and I_o is the average multiplied output current.

Responsivity is a very important parameter for APD characteristics and it can be calculated as follows:

$$R_{\text{APD}} = \frac{I_p}{P(d)}, \tag{7}$$

These APD equations are shown in details with derivation in [25].

A 2D Schrödinger equation is solved as shown in [24] at a suitable portion located at the center of the device when the potential profile is analyzed. In order to obtain the average wave functions $\overline{\xi^m}(y,\, z)$, the following 2D Schrödinger equation is solved for eigen values:

$$\Big[-\frac{\hbar^2}{2}\frac{\partial}{\partial y}\Big(\frac{1}{m_y^*(y,z)}\Big)\frac{\partial}{\partial y} - \frac{\hbar^2}{2}\frac{\partial}{\partial z}\Big(\frac{1}{m_z^*(y,z)}\Big)\frac{\partial}{\partial z} + \overline{U}(y,z)\Big]\overline{\xi^m}(y,z) = \overline{E_{sub}^m}.\overline{\xi^m}(y,z), \tag{8}$$

where,
$\hbar$ is reduced Planck's constant,
$\overline{U}(y,z)$ is average conduction band-edge,
$m_y^*(y,z)$ = effective masses of electron in the y direction,
$m_z^*(y,z)$ = effective masses of electron in the z direction.

After getting the eigenvalues $\overline{E_{sub}^m}$ and eigen functions $\overline{\xi^m}(y,z)$, the subband profile is obtained using first order perturbation theory,

$$E_{sub}^m(x) = \overline{E_{sub}^m} + \oint_{y,z} U(x,y,z)|\,\overline{\xi^m}(y,z)\,|^2 dydz - \oint_{y,z}\overline{U}(y,z)|\,\overline{\xi^m}(y,z)\,|^2 dydz, \tag{9}$$

The shift in absorption lines can be estimated by comparing the energy levels from simulation results obtained in unbiased and biased SAM APDs. It is a simpler task to find the

energy levels using quantum mechanical FUMS approach. If the external electric field is small, it can be considered as a perturbation to the unbiased system and we can invoke perturbation theory to find energy levels for the biased system too.

Stark Effect not only shifts the absorption lines, but also decreases peak absorption coefficient. The external field drives the electrons and holes in the opposite direction and so probability of overlapping is reduced. As transition probability is reduced, peak absorption coefficient decreases. However, it also establishes a control of electric field over light absorption that can be used as an optical modulator. Thus, we can estimate change in absorption coefficient simply by calculating how much separation between electron and holes is increased with the increasing electric field.

III. Results and Discussions

At first, we run the Schrödinger-Poisson solver to obtain valid energy states of InP-InGaAs SAM APDs. We run the solver applying different values for external electric field and for each case, obtain the valid eigen values and sub-bands for electrones and holes. We calculate change in energy gap for peak exciton by taking exciton energy for zero external electric field as reference. Fig. 2 shows the change in exciton peak as we increase external applied field. In the figure, it is clear that this shift is negative, so the peak exciton energy is lowered with applied electric field. The lowering of energy occurs because of Stark Effect. When we apply electric field, it lowers the conduction band minima and raises the valence band maxima. As a result, the gap between them reduces and photon can be absorbed at a lower energy in the InGaAs absorption layer. In the figure, we also find that the shift of peak exciton energy is relatively small for low external electric fields. But at higher applied electric fields, the change is sharp, as the external Stark electric field then dominates the internal depletion layer electric field.

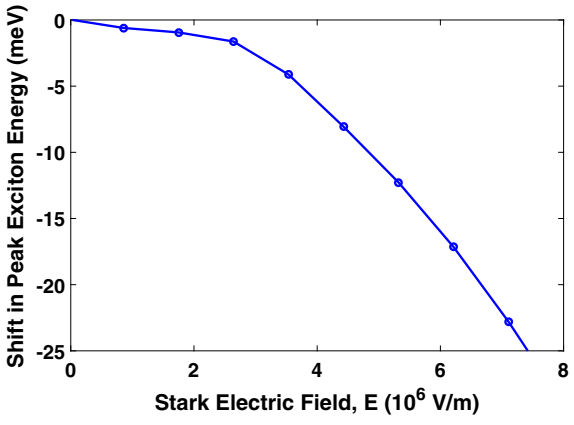

Fig. 2. Peak Exciton Energy Shift vs. Stark Electric Field

To demonstrate the change in absorption coefficient due to Stark Effect, we need to calculate overlapping integral probability for the valence and conduction band in transition of InP-InGaAs SAM APDs. Absorption of photons obviously is less when the overlapping probability becomes lower. In Fig. 3, we show squared normalized overlapping integral values for different external electric fields. At low values of electric field, overlapping probability is very high, almost close to unity. As the applied field is increased, overlapping integral reduces significantly to less than half of its initial value. In this case, peak absorption coefficient will be lowered too. The Stark electric field separates the electrons and holes, it pulls the electrons to the left and holes to the right. As a result, overlapping probability of relating valence and conduction band in transition is decreased and so, absorption coefficient will be lower. However, we see the overlapping probability stops to decrease after a certain higher value of Stark electric field. This is also obvious, as the separation of carriers is limited by the device boundaries.

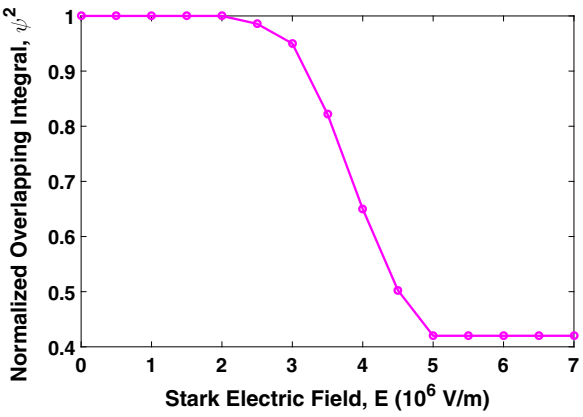

Fig. 3. Normalized Overlapping Integral vs. Stark Electric Field

Fig. 4 shows the variation of absorption coefficient of InP-InGaAs SAM APDs with external Stark electric field. The absorption coefficient for peak exciton value is lowered with external electric field due to Stark Effect. As we discussed earlier, Stark Effect minimizes overlapping probability and so absorption probability also becomes lower. Absorption coefficinet which essentially depicts this probability, is thus shifted to lower value for peak exciton with presence of Stark Effect. Also, we note that the curve is apparently shifted to the left with Stark electric field. This shift means that photons with a lower energy are absorbed in the InGaAs layer for peak exciton with Stark Effect. This confirms our findings in Fig. 2.

Photocurrent variation of InP-InGaAs SAM APDs due to Stark Effect is presented in Fig. 5. In this figure, we find that photocurrent increases when external Stark electric field is applied. This is because of the fact that Stark effect lowers the energy gap and so photon absorption can be done at lower energy as shown in Fig. 2 and Fig. 4. So photons incident with lower energy than the unbiased bandgap and also with higher energy- all get absorbed to give a rise to the photocurrent value. In this figure, we also find that photocurrent peak is shifted to the right along wavelength when Stark Effect

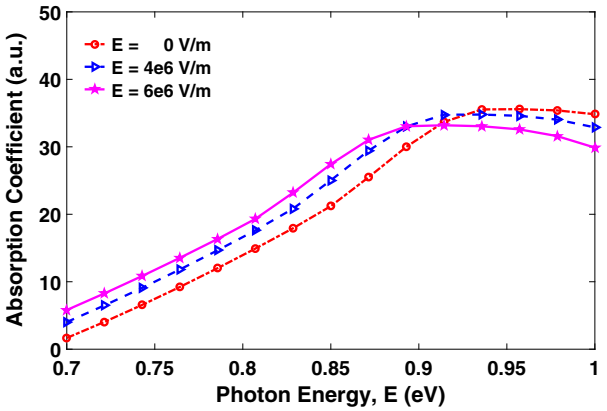

Fig. 4. Variation of Absorption Coefficient with Photon Energy for Different Stark Electric Fields

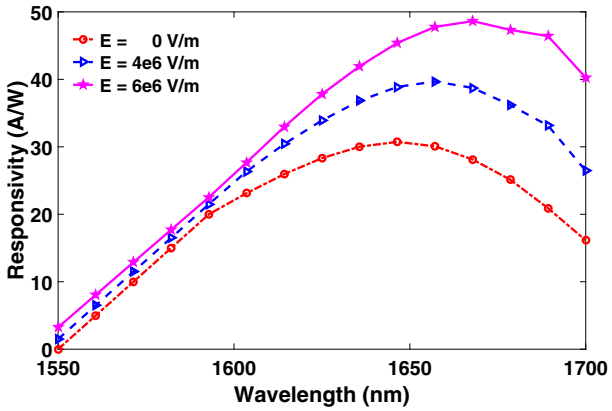

Fig. 6. Variation of Responsivity with Exciton Wavelength for Different Stark Electric Fields

is present. This is another view which confirms that energy gap is lowered and consequently, peak exciton wavelength is increased. However, we see that peak photocurrent loses its oscillatory nature at higher Stark electric field. This is consistent with standard Stark Effect [26]. Thus, we suggest a novel method to control and improve photocurrent of SAM APDs using Stark Effect.

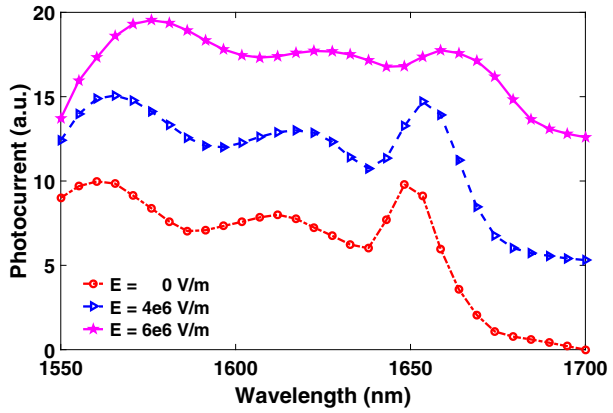

Fig. 5. Variation of Photocurrent with Exciton Wavelength for Different Stark Electric Fields

We present Stark Effect on photocurrent in a different way in Fig. 6 by calculating responsivity using (7). In this figure, it is also clear that for same incident photon energy, responsivity is higher when Stark Effect is present. As responsivity is directly proportional to photocurrent, this figure also confirms our result obtained in Fig. 5. The right shift of the peak responsivity with respect to wavelength is yet another evidence that photon energy required for absorption is lowered when Stark Effect is present.

IV. Conclusion

We have presented Stark Effect on InP-InGaAs SAM APDs and shown different electro-optical shifts with external electrical field. We have shown that photon energy required necessary for absorption can be lowered by applying an external electric field. Then we have calculated absorption coefficient showing overlapping integral probability for the valence and conduction band in transition of InP-InGaAs SAM APDs. Based on the photon energy reduction with Stark Effect, we have presented a novel way to improve photocurrent of SAM APDs. We have shown Stark Effect on photocurrent in terms of responsivity too. Our work can be extended for other APDs and thus, can open ways to design new, efficient and improved optical modulators with high photocurrent that can be extensively controlled by Stark Effect.

References

[1] A. K. Ganguly, A. Ganguly, M. Bhoumic, and A. Ganguly, "High-Speed Metal-Semiconductor-Metal Photo diode," in *Industrial and Information Systems, 2008. ICIIS 2008. IEEE Region 10 and the Third International Conference on*, Dec 2008, pp. 1–4.

[2] H. W. Ruegg, "An optimized avalanche photodiode," *IEEE Transactions on Electron Devices*, vol. 14, no. 5, pp. 239–251, May 1967.

[3] L. Pancheri, M. Scandiuzzo, D. Stoppa, and G. F. D. Betta, "Low-Noise Avalanche Photodiode in Standard 0.35 μm CMOS Technology," *IEEE Transactions on Electron Devices*, vol. 55, no. 1, pp. 457–461, Jan 2008.

[4] D. Dupuy and M. Lescure, "Improvement of the FMCW laser rangefinder by an APD working as an optoelectronic mixer," *IEEE Transactions on Instrumentation and Measurement*, vol. 51, no. 5, pp. 1010–1014, Oct 2002.

[5] P. D. Olcott, J. Zhang, C. S. Levin, F. Habte, and A. M. K. Foudray, "Finite element model based spatial linearity correction for scintillation detectors that use position sensitive avalanche photodiodes," in *Nuclear Science Symposium Conference Record, 2005 IEEE*, vol. 5, Oct 2005, pp. 2459–2462.

[6] M. McClish, K. S. Shah, R. Grazioso, J. Glodo, R. Farrell, E. Karplus, and R. Benz, "A hybrid position sensitive avalanche photodiode detector for scintillation spectroscopy and imaging," in *Nuclear Science Symposium Conference Record, 2003 IEEE*, vol. 2, Oct 2003, pp. 1358–1362 Vol.2.

[7] N. Susa, H. Nakagome, H. Ando, and H. Kanbe, "Characteristics in InGaAs/InP avalanche photodiodes with separated absorption and multiplication regions," *IEEE Journal of Quantum Electronics*, vol. 17, no. 2, pp. 243–250, February 1981.

[8] Y. S. Kim, I. S. Jun, and K. H. Kim, "Design and Characterization of CMOS Avalanche Photodiode with Charge Sensitive Preamplifier," *IEEE Transactions on Nuclear Science*, vol. 55, no. 3, pp. 1376–1380, June 2008.

[9] A. K. Ganguly, A. Ganguly, M. Bhoumic, and A. Ganguly, "High-Speed Metal-Semiconductor-Metal Photo diode," in *Industrial and Information Systems, 2008. ICIIS 2008. IEEE Region 10 and the Third International Conference on*, Dec 2008, pp. 1–4.

[10] D. Allocca, V. M. Contarino, M. F. Squicciarini, and R. I. Billmers, "Evaluation of 8×8 reverse etched avalanche photo diode arrays for oceanographic lidar systems," in *OCEANS '95. MTS/IEEE. Challenges of Our Changing Global Environment. Conference Proceedings.*, vol. 2, Oct 1995, pp. 1168–1173 vol.2.

[11] G. M. Williams, D. A. Ramirez, M. Hayat, and A. S. Huntington, "Discrimination of Photon- and Dark-Initiated Signals in Multiple Gain Stage APD Photoreceivers," *IEEE Journal of the Electron Devices Society*, vol. 1, no. 4, pp. 99–110, April 2013.

[12] B. T. Vu, N. T. Dang, T. C. Thang, and A. T. Pham, "Bit error rate analysis of rectangular QAM/FSO systems using an APD receiver over atmospheric turbulence channels," *IEEE/OSA Journal of Optical Communications and Networking*, vol. 5, no. 5, pp. 437–446, May 2013.

[13] M. Pous and F. Silva, "Full-Spectrum APD Measurement of Transient Interferences in Time Domain," *IEEE Transactions on Electromagnetic Compatibility*, vol. 56, no. 6, pp. 1352–1360, Dec 2014.

[14] X. Liang, Z. Su, and S. Bi, "Research on the associated feature of APD sensor avalanche gain and photoelectric conversion SNR," in *Fuzzy Systems and Knowledge Discovery (FSKD), 2012 9th International Conference on*, May 2012, pp. 1913–1916.

[15] D. A. Luong, C. T. Truong, and A. T. Pham, "Effect of APD and thermal noises on the performance of SC-BPSK/FSO systems over turbulence channels," in *Communications (APCC), 2012 18th Asia-Pacific Conference on*, Oct 2012, pp. 344–349.

[16] J. M. T. Pereira, "Light effects on the frequency response of InGaAs/InP SAM-APD devices," in *Electrotechnical Conference, 2004. MELECON 2004. Proceedings of the 12th IEEE Mediterranean*, vol. 1, May 2004, pp. 15–18 Vol.1.

[17] K. Wakita, I. Iotaka, K. Mogi, H. Asai, and Y. Kawamura, "High-speed AlGaInAs/AlInAs multiple quantum well pin photodiodes," *Electronics Letters*, vol. 25, no. 22, pp. 1533–1534, Oct 1989.

[18] J. Waclawek, J. Kovac, B. Rheinlander, V. Gottschalch, and J. Skriniarova, "Electrically tunable GaAs/AlGaAs MQW RCE photodetector," *Electronics Letters*, vol. 33, no. 1, pp. 71–72, Jan 1997.

[19] M. R. Abbasi, M. H. Sheikhi, and A. Zarifkar, "Circuit model simulation for separate absorption, grading and multiplication avalance photodiodes (SAGM-APD) considering gradual changes of the electric field in active region," in *Information and Communication Technology in Electrical Sciences (ICTES 2007), 2007. ICTES. IET-UK International Conference on*, Dec 2007, pp. 862–868.

[20] Y. H. Kuo, Y. K. Lee, Y. Ge, S. Ren, J. E. Roth, T. I. Kamins, D. A. B. Miller, and J. S. H. Jr., "Quantum-Confined Stark Effect in Ge/SiGe Quantum Wells on Si for Optical Modulators," *IEEE Journal of Selected Topics in Quantum Electronics*, vol. 12, no. 6, pp. 1503–1513, Nov 2006.

[21] F. Mayer, "Stark effect produced frequency shifts in the helium-neon laser," *IEEE Journal of Quantum Electronics*, vol. 3, no. 12, pp. 690–691, Dec 1967.

[22] Y. Wang and K. F. Brennan, "Theoretical study of a classically confined solid-state photomultiplier," *IEEE Journal of Quantum Electronics*, vol. 26, no. 10, pp. 1838–1844, Oct 1990.

[23] K. Safa, *Optoelectronics and Photonics: Principles and Practices*. Pearson Education India, 2009.

[24] J. Wang, E. Polizzi, and M. Lundstrom, "A three-dimensional quantum simulation of silicon nanowire transistors with the effective-mass approximation," *Journal of Applied Physics*, vol. 96, no. 4, pp. 2192–2203, 2004.

[25] G. Keiser, *Optical Fiber Communications*. John Wiley and Sons, Inc., 2003.

[26] H. Wang, P. LiKamWa, M. Ghisoni, G. Parry, P. N. Stavrinou, C. Roberts, and A. Miller, "Ultrafast recovery time in a strained InGaAs-AlAs p-i-n modulator," *IEEE Photonics Technology Letters*, vol. 7, no. 2, pp. 173–175, Feb 1995.